

TUNEABLE EMITTANCE THIN FILM COATINGS FOR THERMAL CONTROL

E. Haddad⁽¹⁾, R. Kruzelecky⁽¹⁾, B. Wong⁽¹⁾, W. Jamroz⁽¹⁾, M. Soltani⁽²⁾, M. Chaker⁽²⁾, M. Benkahoul⁽²⁾, P. Poinas⁽³⁾

⁽¹⁾ MPB Communications, 151 Hymus Boulevard; Montreal, Quebec, Canada H9R-1E9,
Phone (1) 514 694 8751 Email: Emile.haddad@mpbc.ca

⁽²⁾ INRS-EMT 1650 Boulevard Lionel Boule, Varennes, Quebec, Canada J3X-1S2

⁽³⁾ ESA ESTEC, PB 299; 2200 AG, Noordwijk; The Netherlands

ABSTRACT

Passive thermal control systems are important to reduce the power budget and cost of space missions and satellites.

MPB has developed advanced technologies, based on $V_{1-x-y}M_xN_yO_n$ thin films, for the passive dynamic thermal control of space structures and payloads. A main challenge is to decrease the net solar absorptance (α), while maintaining high emittance tuneability. The approach uses a relatively simple thin dielectric stack reflector based on SiO_2 (e.g. $SiO_2(\lambda/4)/VO_2(\lambda/4)$) to provide peak reflectance at $\lambda=500$ nm, the spectral position of the peak solar AM0 radiation. Depositing each of these additional layers may interfere with the original properties of the lower layers, changing their residual stresses and morphology. This is a major challenge for all the technologies based on multilayer thin or thick films proposed as tuneable emittance devices.

These films, in preparation for a technology flight demonstration, have successfully passed major ground tests and its performance has been validated for extended use in the harsh space environment, with a target of up to 15 years GEO. The developed Vanadium dioxide based thin film technology is versatile. MPB has deposited VO_2 films on Kapton for use as a sunshield for antenna membranes. The VO_2 films have been shown to be very flexible and suitable for curved surfaces and therefore may be considered for thermal control of astronaut suits. They can be used to assist in thermal control in order to maintain equipment within their operational temperatures limits by opposing the effects of temperature swings in Lunar exploration or Mars missions. This paper reviews the current status of MPB's smart radiator and its validation for efficient thermal control using the tuneability of its thermo-optic properties.

1 INTRODUCTION

Efficient thermal control of a spacecraft is an important issue that impacts on the performance and longevity of the internal subsystems. Spacecrafts are subjected to external temperature swings from about -150°C to $+150^\circ\text{C}$. However, the corresponding internal temperature must be regulated over 0 to 40°C . Current dynamic thermal-control systems employ mechanical louvers consisting of vanes or windows that are opened and closed to regulate the radiation to dark space [Gilmore 1994]. With the trend towards

higher functional densities per unit mass on satellites and longer mission life, there is a need for a more-efficient, cost-effective, reliable thermal control system. Figure 1 presents the effects of the emissivity on the spacecraft internal temperature. A low IR emissivity such as Al (0.05) keeps the internal temperature above -10°C even at a reduced heat load (2.3 W/m^2), i.e. when the radiator is facing the shadow. However, tripling the heat load (7.4 W/m^2) will increase the temperature above the nominal operational limit of about 50°C . At the other extreme, a high emissivity (0.9) will dissipate a heat load up to $150 \text{ (W/m}^2\text{)}$ before the radiator reaches the limit of 50°C . However, the radiator temperature will go below -10°C , even at an elevated heat load of 60 W/m^2 , thus requiring an internal heater to protect the payloads.

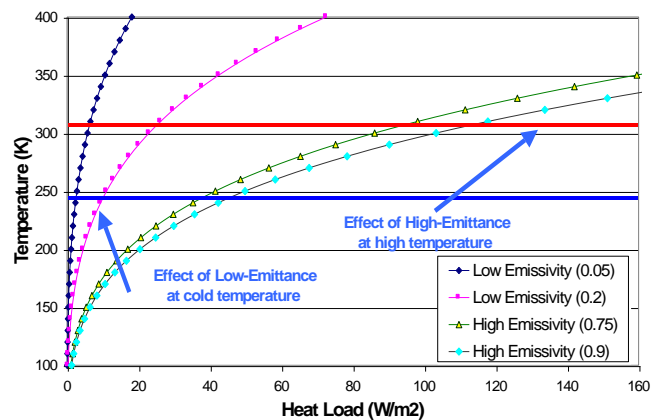


Figure 1: Emissivity effect on the variation of the radiator temperature due to the heat load

An Ideal smart radiator device (SRD) would have a low emittance at lower temperatures, and a high emittance at high temperatures, thus maintaining the internal payloads at a moderate temperature under varying conditions. Broad IR emittance tuneabilities exceeding 0.45 have been achieved. This dynamic emittance tuneability can provide a substantial improvement in the thermal stability of the space structure for varying operating conditions, while significantly reducing or eliminating the need for auxiliary heaters during spacecraft cold swings. The SRD should reduce the peak-to-peak temperature swings of the spacecraft. This would enable existing space systems to operate in temperature ranges of maximum performance. Thin-film coating (V_{1-x}

$yM_xN_yO_n$) can be applied to existing thermal blankets such as Kapton and Teflon FEP, or to thermal radiators such as Al, to facilitate dynamic thermal control. This approach employs the metal–insulator transition to control the heat dissipation and has significant advantages in terms of weight, cost, integration with the space structure, and structural simplicity.

A few other miniaturization methods are actually being developed:

- LaSrMnO₃ thin or thick films that show a phase transition from ferro-magnetic metal to paramagnetic insulator at around room temperatures. The transition is attributed to the double exchange effects [Zener 1951, Tachikawa 2009]
- Electrochromic structures based on WO₃ exhibit relatively low VIS/NIR optical absorption in the insulating state and a high reflectance in the metallic state [Frannke 2001, Metts 2009].
- Micromachined louver systems fabricated on Si using MEMS technologies. These devices are similar in function and design to conventional mechanical louvers [Magna 2008].
- Miniaturized heat pipes, where the mechanically pumped cooling system consists of a working fluid circulated through microchannels by a micropump [Birur 2001].
- Electrostatic force to pull two surfaces very close to increase the thermal conductivity between them. This technique requires high DC voltage (> 100 V), and is more suitable for thermal switch application [Bitter 2003].

The two first approaches based on thin films are presented in Section 6.

2 METAL–INSULATOR TRANSITION

Several material systems have been identified that can exhibit a change from metallic to insulator behaviour (metal-insulator transition) in response to composition (doping), electric field, temperature, or the application of pressure. These mechanisms can cause a change in the electron occupancy of allowed band levels to shift the Fermi energy from forbidden or localized levels (non-metallic behavior) to extended conduction states (metallic behavior).

Metals are characterized by valence electrons in partially filled bands with extended wavefunctions that can contribute to electronic and thermal conduction. The corresponding Fermi energy, E_F , which describes the electron occupancy statistics, lies within the partially filled energy band. The resulting high density of free electrons results in the characteristic high optical reflectivity and of most metals and corresponding low thermal emissivity ($\epsilon < 0.2$). In contrast, the valence electrons of insulators are localized in a filled valence band (at 0 K) that is separated by a quantum-mechanically forbidden band

gap, E_g , from a largely unoccupied conduction band. In this case, the Fermi energy lies within the forbidden band gap. Photons with energies below E_g are transmitted by the insulator, while photons with energies above E_g are absorbed by the valence electrons, facilitating electron transitions to the conduction band. Insulators are characterized by conductivities that increase exponentially with temperature and relatively high thermal emissivities ($\epsilon > 0.5$).

Many of the transition metals such as W, Mn, La, and V, are characterized by partially-filled d-orbitals which contribute to metallic bonding and electrical conduction. The transition metals can readily form a variety of complexes involving the d-orbitals [Mahan 1975]. The energy splitting of the d-orbitals due to the formation of the chemical complex results in an effective band-gap, for optical absorption and conduction. As the temperature increases, electrons from filled lower d-orbitals are promoted to the empty orbitals at higher energies, resulting in conduction electrons and holes.

VO_n exhibits one of the largest observed variations in electrical and optical characteristics due to the metal-insulator transition. The transition temperature increases with the oxygen content, varying from 126 K for VO, to 140K for V₂O₃, and to 341 K for VO₂ [Griffith 1974]. The metal-insulator transition in V_xO_n is associated with a change in structure from a tetragonal rutile structure with metallic characteristics above the transition temperature to a monoclinic structure with insulator-like characteristics below the transition temperature. The transition temperature varied between 58 and 68°C, depending on the O₂ partial pressure. These results indicate that the metal-insulator transition characteristics of thin VO₂ films can be comparable to those of bulk samples. Stefanovich et al. observed the field-induced switching in the electrical resistivity of VO₂ in a metal-oxide-semiconductor electrical field-effect configuration. It indicates that the metal-insulator transition in VO₂ is related to a critical electron density, similar to the classical Mott metal-insulator transition [Stefanovich 2000]. The Mott criteria for the transition is given by:

$$(n_c)^{1/3} r_H \approx 0.25,$$

where n_c is the critical electron density and r_H is the Bohr radius. The value of the critical density was found experimentally [Stefanovich 2000] to be about $3 \cdot 10^{18} \text{ cm}^{-3}$, in good agreement with theoretical predictions. Based on the VO₂ switching behavior in transistor structures, estimates of the metal-insulator transition cycling in VO₂ exceed 10^8 cycles [Beteille 1998]. Since the driving mechanism is an electric field effect, the power requirements will be moderate.

The VO₂ tuneability was demonstrated in various methods offering a flexibility to select the way to induce the transition (Table 1).

Table 1: Methods of VO₂ Switching

Method to induce the transition	Comments and references
Thermally induced transition (called passive)	Transition time a few minutes First MIT experiments [Morin 1959] Thin film on Si, SiO ₂ [e.g. Guinneton 2004] and on Al substrate [Kruzelecky 2005]
Photonic	Very fast Transition <100 fs High power Laser pulses (x-rays or visible) [Cavalleri 2001, Baum 2007]
Mixed Photonic/Thermal (the laser is contributing to heat the VO ₂ film)	Transition time ~1 μs to ~1 ms - Pulsed NdYAG 1064 nm >1 mJ/cm ² [Chudnovskii 1999] - CW HeNe 632 nm: 2 mW or 1 mJ/cm ² [Egorov 1991, a, b, c]
Slow Electrical switch	Sol gel prepared VO ₂ Film ; slow switching ~1 minute [Dchuan 1996]
Fast Electrical switching (charge injection)	Very fast 1.5 ns [Stefanovich 2000] depends on the VO ₂ -deposition and MEMs structure

3 VO₂ PREPARATION AND CHARACTERIZATION

The VO₂ layers were grown on specially-prepared Al. Additional substrates such as crystalline silicon and quartz were utilized to assist in the characterization of the films

3.1 Film Preparation

Undoped and doped VO₂ films were prepared in a s.s. vacuum chamber by reactive pulsed laser ablation using a special target and a KrF excimer laser in a portable clean room at MPB (Figure 2) [Kruzelecky 2005]. The depositions were performed in a controlled gas-phase background consisting of an O₂/Ar gas mixture at total pressures of 100 mTorr. The substrate temperature was typically held at about 500°C.

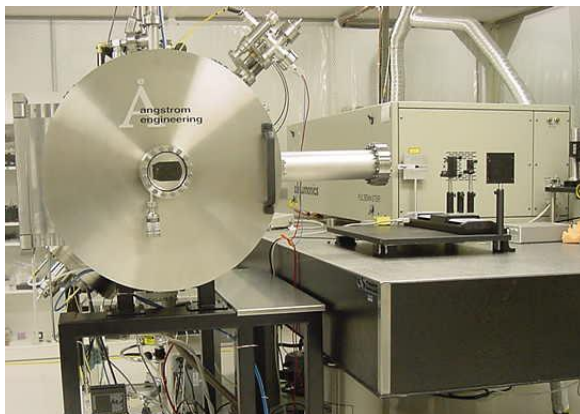


Figure 2: Photograph of advanced high-vacuum, reactive laser-ablation deposition facility at MPB

3.2 Film Characterization

X-ray diffraction (XRD) was employed to study the structure and stoichiometry of the resulting coatings. It indicated that high-quality VO₂ could be deposited on crystalline substrates, on sapphire, as well as its on Al (Figure 3). This is very advantageous for the current application since the smart coating can be directly deposited on the desired radiator surface to maximize heat transfer and mechanical integrity of the SRD while minimizing the overall SRD weight. The detailed characterization was presented in a previous paper [Kruzelecky 2005]

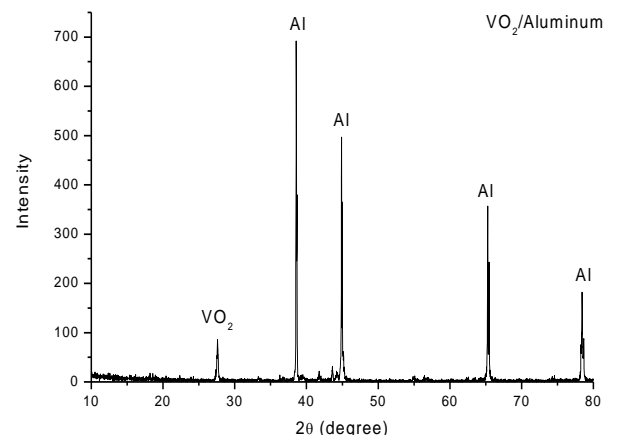


Figure 3: X-ray diffraction spectra of VO₂ deposited onto polished Al.

VO₂ deposited on a low emissivity substrate such as polished Al exhibits a low emissivity in the semiconductor or insulating state at lower temperatures ($\epsilon_{net} < 0.25$) due to the high IR, with increase in the emittance around 70°C, corresponding to the formation of free electrons in the controlled semi-metallic state. Figure 4 illustrates the granular shape of a 240 nm thick VO₂ film on Al-substrate.

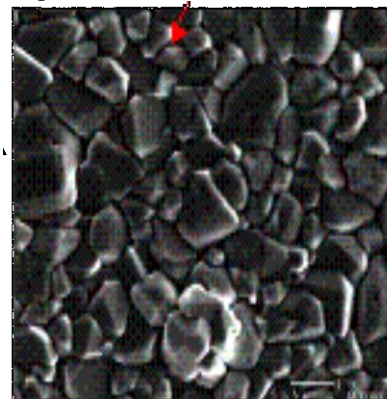


Figure 4: Picture of the Scanning Electron Microscope (SEM), of the VO₂ film.

MPB's approach uses a standardized smart radiator tile measuring 20 x 20 mm or 40 x 40 mm. The tile can be affixed to the current honeycomb or other

radiator panels to provide smart radiators of various sizes as required.

With nano-texturing of the Al substrate, the VO₂ film creates a semi metallic surface that behaves differently from VO₂ films on insulator substrates (e.g. SiO₂), Figure 5 and Figure 6. On the Al surface the VO₂ has low emittance (high reflectance) at lower temperature, whereas the emittance increases after the transition (low reflectance) at high temperature.

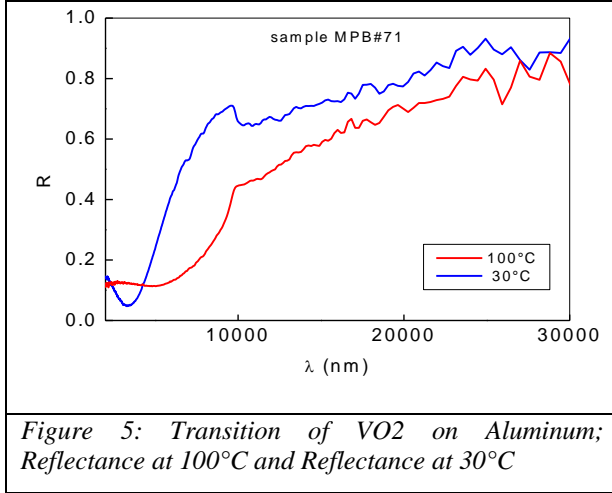


Figure 5: Transition of VO₂ on Aluminum; Reflectance at 100°C and Reflectance at 30°C

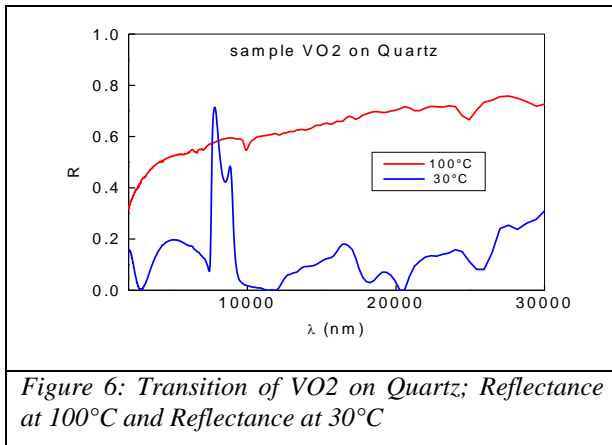


Figure 6: Transition of VO₂ on Quartz; Reflectance at 100°C and Reflectance at 30°C

Table 2 summarizes the attained dynamic variation in thermal emittance for a VO₂-based SRD. Net emittance tuneabilities of $\Delta\epsilon=0.45$ have been experimentally measured for simple, single layer structures

Table 2: Summary of the preliminary characteristics for VO_n-based thin-film SRDs.

Radiator Temperature Switch Point	Low Temperature Emissivity	High Temperature Emissivity
-20°C to >70°C	0.2 to 0.3	0.55 to 0.75

3.3 Doping

VO₂ in the insulating state is a semiconductor that can be doped with suitable donors and acceptors to tailor its characteristics. This is a major advantage of the VO₂-based material system and facilitates a strong spin-off potential for other micro/nano technology applications. Impurities such as W and Mo provide an extra d-orbital electron relative to the Vanadium, acting as donors. Impurities such as Ti, with one fewer d-orbital electron than V, act like classical acceptors.

Table 3 summarizes experimental results for doped VO₂. The metal-insulator transition temperature exhibited by VO₂ can be shifted over a wide range, from above 70°C to below -20°C, as may be required.

Table 3: Effect of W and Ti doping on the metal-insulator transition temperature of VO₂

W-doping	0.0	1.5%	3%	3%
Ti Doping	0.0	0%	0%	1%
Mid-Transition Temperature	68°C	37°C	-20°C	0°C

Preliminary W-doped VO₂ samples were prepared on textured Al using both 1.5% W and 2% W doping. Preliminary results are summarized in Table 4. For 1.5% W doping of the VO₂, the transition from low to high IR emittance started at about 28°C, with ϵ (high) being reached at about 60°C (sample SRD96). Increasing the W doping to about 2%, reduced the ϵ (low) to ϵ (high) transition temperature below 20°C. The results on doping of the VO₂ films indicate that there is considerable flexibility to tailor the thermo-optic and switching characteristics of VO₂ films. Co-doping with Ti can be used to improve the optical transmittance characteristics of the VWTiO₂ in the insulating state and fine-tune the transition temperature width.

Table 4: Preliminary results of 1.5% W doping on metal-insulator transition temperature of VO₂

Sample	ϵ (low)	Transition Temperature Range	ϵ (high)	$\Delta\epsilon$
SRD74 (undoped)	0.26 (T<55°C)	55 to 75 °C	0.60 ((T>70°C)	0.34
SRD96 (1.5% W doped)	0.23 (T<30°C)	28 to 60 °C	0.57 (T>65°C)	0.34
SRD84 (2% W doped)	Not measured (Condensation)	Below 20 °C	0.6 (T>20°C)	

Figure 7 illustrates the Infrared transmittance FTIR (2.5 μ m) as a function of increasing temperature for undoped VO₂, W doped and W-Ti doped thin films deposited on quartz substrates ($x=0.014$, $y=0.12$).

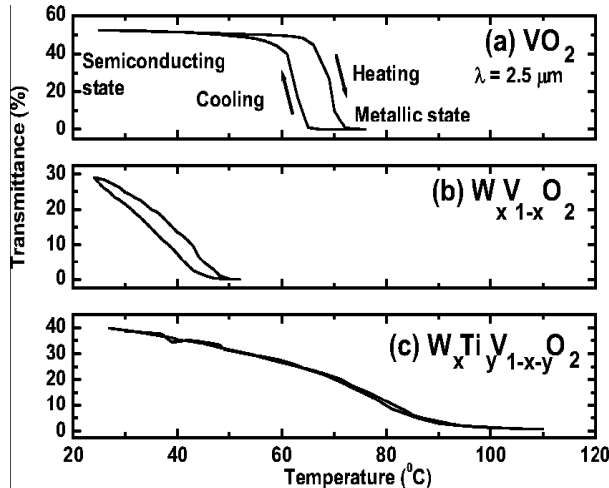


Figure 7: Infrared transmittance FTIR as a function of increasing temperature for a) VO_2 , b) $V_{1-x}W_xO_2$ and c) $V_{1-x-y}W_xTi_yO_2$ thin films deposited on quartz substrates; at $4000\text{ cm}^{-1} \sim 2.5\ \mu\text{m}$ ($x=0.014$, $y=0.12$).

4 MONOLAYER SPACE ENVIRONMENT TESTING

Preliminary ground testing of VO_2 based thin film smart radiator devices (SRD) showed that the films could withstand the space environment conditions of a Geo satellite with a lifetime of 15 years, including the harsh launch conditions (vibrations and shock). Table 5 shows a list of the tests performed, with the corresponding applied test standard.

Table 5: List of the performed tests, with the applied standard and the laboratory that performed the test.

Test Series	Test Description and Reference
Humidity-storage	4 cycles 2-35°C, 90% Relative Humidity, for 36 hours [ECSS-E-10-03A]
Sinusoidal Vibration	Between 5 and 100 Hz, 13 g for 18 to 35 Hz [ECSS-Q-70-04A]
Random Vibration	Between 100 and 2000Hz, RMS 15g [ECSS-Q-70-04A]
Shock (Thermal)	11 cycles between $-196\text{ }^\circ\text{C}$ (LN2) and $165\text{ }^\circ\text{C}$ [MIL-STD-883E]
Accelerated Aging	8200 vacuum cycles between -15° and $+80^\circ\text{C}$, simulating 15 years GEO (x 1.5 security factor) [ECSS-Q-70-04A]
Thermal cycling	39 vacuum cycles between -150° and $+150^\circ\text{C}$ [ECSS-Q-70-04A]
Adhesion to radiator	Adherence strength of 670 N/cm [ECSS-Q-70-13A]
VUV and ATOX	Preliminary Test AO-VUV, equivalent to 3 years LEO Radiation.

The test series is considered as one global test, to analyze the SRD capability to withstand the harsh space environment for the equivalent of 15 years geosat. The VUV-atomic oxygen and the radiation tests are preliminary and were applied on separate coupons. The results of three samples (i.e. MPB-38, MPB-39 and MPB-40) that passed through the test series are discussed below.

4.1 Emittance

Figure 8 a), b) and c) present a summary of the emissivity of the delta emittance (difference between the SRD high-emittance and low-emittance) for different environmental test conditions. The graphs illustrate the evolution of the three samples (MPB-38, MPB-39 and MPB-40) within the test series; including humidity, vacuum accelerated aging (8,200 cycles, from -15°C to $+80^\circ\text{C}$), sinusoidal and random vibrations, thermal vacuum cycling (39 cycles between -150°C and $+150^\circ\text{C}$) and thermal shock (11 cycles between -195°C and 165°C). Figure 8 shows that the delta emissivity ($\Delta\varepsilon = \varepsilon_{\text{High}} - \varepsilon_{\text{Low}}$) stays constant, with no significant variation. The variations in $\Delta\varepsilon$ were less than ± 0.03 , and the average of the three samples varied less than ± 0.01 . The measurement accuracy is approximately ± 0.02 .

There are some small fluctuations in the Low emittance and High emittance (Figure 8 b, c). These fluctuations may be caused by small variation of the room temperature that changes the value of total heat proportional to $\varepsilon(T^4 - T_{\text{ambient}}^4)$ and hence the deduced value of the absolute emittance. The room temperature could fluctuate between 20 and 23°C , but was not registered. Nevertheless, the average variation of the low and high emittance, for the three tested samples, is less than 0.02.

4.2 Solar Absorptance

The hemispherical reflectivity of a 150 nm single-layer VO_2 SRD (MPB-39) relative to Al substrate, was measured before and after the test series. The solar absorptance was relatively high about 0.4 and increased to 0.45. after the tests.

4.3 VUV Atomic Oxygen

The mass loss efficiency of the VO_2 film for reactions with atomic oxygen is very low, comparable in fact to that of the SiO_2 ($<0.8 \times 10^{-27}\text{ cm}^3/\text{at}$) that is employed as an AO-protective coating. The results indicate that the surface erosion of the VO_2 coating by atomic oxygen is rather limited and that the VO_2 can actually offer some AO protection to space surfaces.

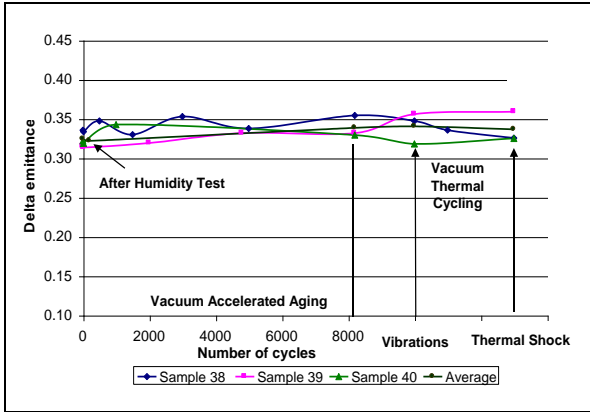


Figure 8 a: Evolution of Emittance Tuneability during the test series.

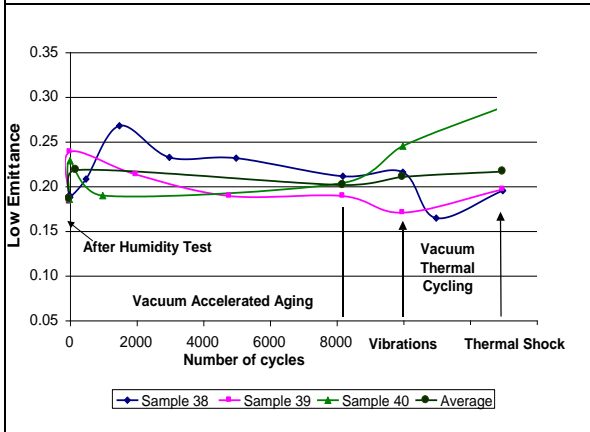


Figure 8b: Evolution of Hemispherical Low-Emittance during the test series

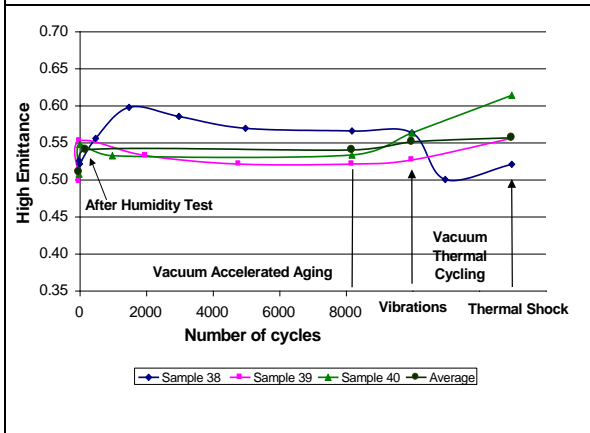


Figure 8c: Evolution of Hemispherical High-Emittance during the test series.

5 MULTILAYER VO₂ BASED SRD

The previous tests, using a single VO₂ thin film on the prepared Aluminum substrate demonstrated the suitability of the SRD for LEO and GEO space environments. To ensure it is competitive with current commercial radiators, it is beneficial to increase the SRD high emittance, and reduce the solar absorptance. The increase of the low emittance can be tolerated, if the tuneability ($\Delta\epsilon$) is not decreased. In parallel, solar absorptance should be reduced further; this can be accomplished by adding selective-

reflectance $\lambda/4$ interference layers for $\lambda=500$ nm (the wavelength of the peak solar radiation).

Table 6 illustrates the main requirements to optimize the SRD thermo-optical, mechanical and electrical properties and the methodology to perform them.

Table 6: Optimization of the SRD properties

Parameter	Requirement	Methodology
Optimize low and high emittance	Increase both low and high emittance with increasing $\Delta\epsilon$	Selection of texturized substrate surface SiO ₂ high emittance overlayer.
Temperature range of tuneability	-10°C to +30°C	Doping with W and Ti
Reduce solar absorptance	<0.25	SiO ₂ /VO ₂ , $\lambda/4$ stack Layer
SRD film mechanical flexibility	Flexible for curved surfaces (astronaut suits)	Intrinsic property to the VO ₂ /SiO ₂ layers

To achieve the challenging requirements, a multi-layer SRD is proposed. The multi-layer SRD is based on a basic structure of tailoring the emittance and solar reflectance, to which additional layers could be added. The multi-layer basic structure could contain (Fig. 9):

- Layer 0: Substrate- polished/textured Aluminium,
- Layer 1: thin vacuum evaporated Ag to reduce net solar absorptance relative to bare Al,
- Layer 2: W-doped VO₂, 150 to 250 nm thick,
- Layer 3: SiO₂ VO₂, ($\lambda/4$) to increase the solar reflectance near 500 nm,
- Layer 4: W-doped VO₂, ($\lambda/4$) to increase the solar reflectance near 500 nm,
- Layer 5: SiO₂, ($m\lambda/n(\text{SiO}_2)$) thick) to shift net emissivity upwards,
- Layer 7: thin W-doped VO₂.

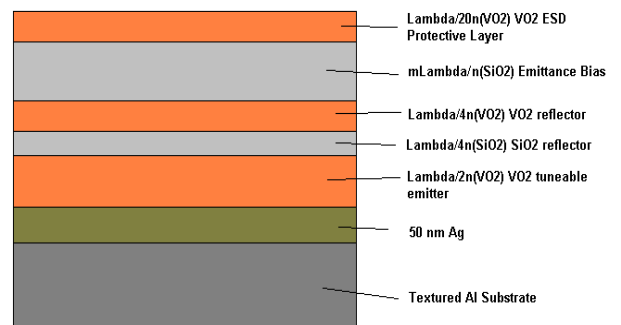


Figure 9: Infrared Schematic of Multilayer VO₂-based SRD.

Figure 10 shows the simulated VIS/NIR optical reflectance for the multilayer structure in Figure 9. The peak reflectance near 0.5 μm can exceed 85% with suitable selection of the layer thicknesses. For the SiO_2 , a refractive index of 1.45 was assumed.

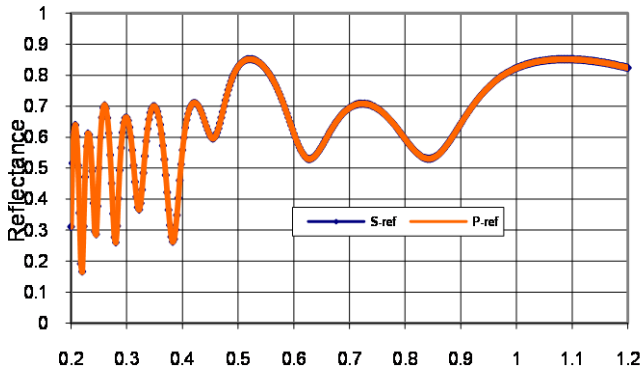


Figure 10: Zeemax simulation of net reflectance of multilayer VO_2 -based SRD shown in Fig. 9.

To achieve a solar absorptance (α) < 0.3 on an opaque substrate such as Al requires a corresponding high net surface reflection in the visible spectral range since

$$\alpha(\lambda) = 1 - R_{\text{dif}}(\lambda) - R_{\text{spec}}(\lambda),$$

where: R_{dif} is the diffuse reflection, R_{spec} is the specular reflection and λ is the wavelength. Since the developed SRD is formed by very thin films whose thickness are less than the wavelength of light to reflect, the reflection of these films will rely on the principles of interference. This can be achieved using a $\text{VO}_n/\text{SiO}_x/\text{VO}_n$ multi-layer reflector of appropriate quarter-wave layer thickness (Layer thickness = $\lambda p/(4n)$, where n is the refractive index of the layer and λp is wavelength corresponding to the solar radiation peak intensity, about 500 nm). The structure alternates the high-index VO_n layer ($n=2$) with the selected low-index layer (SiO_2 , $n=1.4$ to 1.5). Each interface contributes to increase the reflection of the incident solar radiation. Several structures have been simulated using non-sequential Zeemax optical simulation software (see Figure 10). The goal is to minimize the thickness of the individual VO_2 layers to reduce absorptance of the incident solar radiation. The thin Ag coating on the Al is proposed to further decrease the attainable solar absorptance relative to the Al substrate. Figure 11 are results of the initial trial to shift the maximum reflectance by changing the SiO_2/VO_2 stack layer with about 5-10 nm, which is the limit of the deposition measurements accuracy. The SiO_2 was deposited on top of the VO_2 by Plasma Enhanced Chemical Vapor Deposition (PECVD) at Ecole Polytechnique de Montreal, using a mixture of silane SiH_4 and O_2 , with a working pressure of 80 mTorr and an RF power of 100 W. During the deposition a witness etalon of Silicon was included in the vacuum chamber, very close to the samples, to monitor the deposited SiO_2 thickness and its refractive index. This provides SiO_2 with a refractive index near 1.45.

Table 7 compares the solar reflectance of the preliminary multi-layer SRD (one stack SiO_2/VO_2), with a single layer VO_2 sample (SRD 39).

Table 7: Comparison of sample emittance and solar absorptance with addition of VO_2/SiO_2 overlayer.

Sample	$\epsilon(\text{low})$	$\epsilon(\text{high})$	$\Delta\epsilon$	Solar Abs.
Original SRD90 240 nm VO_2/Al	0.34	0.68	0.34	0.57
SRD90C $\text{VO}_2/\text{SiO}_2/240\text{nm}$ VO_2/Al	0.38	0.74	0.36	0.32

The added SiO_2/VO_2 stack provided a substantial improvement in the solar reflectance for the relatively thick VO_2 underlying layer. There is a net overall increase in the IR emittance of about 0.04 that is desirable to reduce the sizing of the radiator.

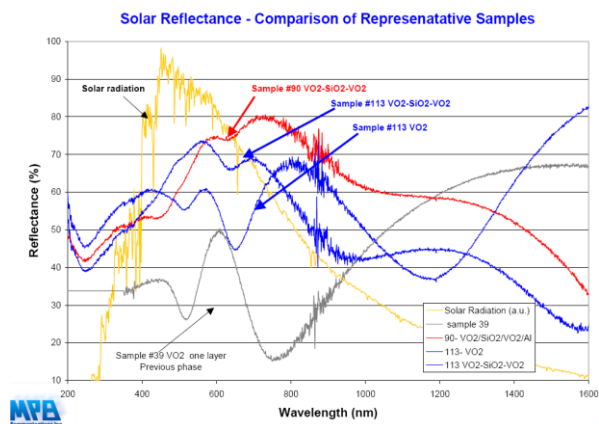


Figure 11: Preliminary results of improving the solar reflectance with SiO_2/VO_2 additional layer.

Figure 11 shows the peak solar reflectance is slightly shifted from that of the solar radiation (A_m0). The main challenge is to maintain a high reflectance and match the peak with that of the solar radiation (around 500 nm), without reducing the emittance tuneability. Further experiments are being performed to continue the optimization

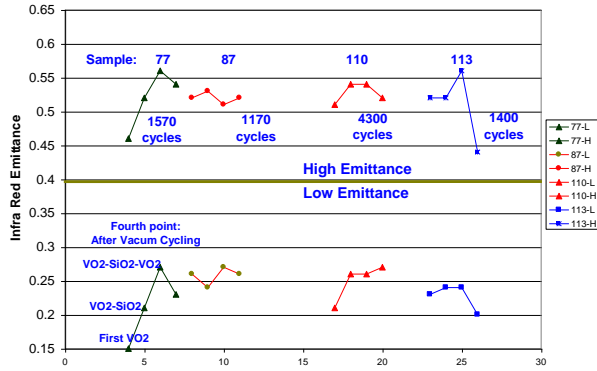
5.1 Fine Tuning the IR Emittance

For a given tuneability $\Delta\epsilon$, a higher emittance will dissipate a greater heat load (Figure 1). Moreover, in space environment it is much more convenient to heat internal parts to reach their functional temperature range, than to cool them from a hot temperature. Hence, for a given $\Delta\epsilon$, it is more desirable to have tuneable radiator at higher ϵ_{High} and ϵ_{Low}

The aim is to increase both the lower and higher emittance without decreasing the tuneability $\Delta\epsilon$. There are two parallel approaches:

1. Select the Al substrate texturing and VO₂ thickness to optimize $\Delta\epsilon$ and add Ag layer over the Al to minimize substrate IR emittance,
2. Add additional VIS transparent fixed emitter layer (SiO₂ of selected thickness) over the VO₂ structure to shift both ϵ_{High} and ϵ_{Low} higher to obtain the desired ϵ_{High} .

Figure 12 illustrates the evolution of ϵ_{Low} and ϵ_{High} of four samples (#77, 87, 110, 113) after the deposition of the first VO₂ layer, after the deposition of the stack layer, after 1400 thermal cycles (10C to 90C) and 17 thermal shock cycles (-196C to +160C). Optimization of the deposition parameters for SiO₂ and VO₂/SiO₂ multilayer design is ongoing with an emphasis on increasing the high temperature emittance without



penalizing the net emittance tuneability.

Figure 12: Preliminary results of improving the solar reflectance with SiO₂/VO₂ additional layer.

Table 8 compares the evolution of the tuneability $\Delta\epsilon$ after each step during the manufacturing and the space environment test. There is a slight decrease of tuneability between the deposition of the first VO₂ layer and the last test.

Table 8: Evolution of emittance tuneability with the space environment testing.

Emittance Tuneability ($\Delta\epsilon$)	Tuneability Average For 5 samples
First layer VO ₂	0.28 ± 0.02
VO ₂ -SiO ₂	0.28 ± 0.02
VO ₂ -SiO ₂ -VO ₂	0.27 ± 0.02
After Thermal Cycling	0.26 ± 0.02

After Thermal Cycling and Thermal shock	0.25 ± 0.03
---	-------------

Table 9 compares the results obtained with the objectives of a commercial smart radiator

Table 9: Comparison of sample emittance and solar absorptance with addition of VO₂/SiO₂ overlayer

Parameter	Objective	Results and Comments
High Emittance (ϵ -high)	> 0.7	Sample #90 (ϵ -high = 0.74) Average (ϵ -high BOL*) = 0.55 Average (ϵ -high EOL**) = 0.58
Low Emittance (ϵ -low)	≤ 0.5	Yes for all samples Average (ϵ -low BOL) = 0.22 Average (ϵ -low EOL) = 0.23
Tuneability (Delta emittance, $\Delta\epsilon$)	≥ 0.35	Yes for one layer Average ($\Delta\epsilon$ -BOL) = 0.27 Average ($\Delta\epsilon$ -EOL) = 0.25
Solar absorptance EOL (α -EOL)	< 0.3	Very close Average (α -BOL) = 0.33 Average (α -EOL) = 0.34

*BOL refers to the results obtained before the tests
**EOL refers to the results obtained after the thermal cycling and thermal shock tests.

6 COMPARISON WITH OTHER TECHNOLOGIES

Two alternative and successful methods of thermal control are being developed the electrochromic effect and thick-film ceramic tiles based perovskite materials.

La_{1-x}M_xMnO_n is a class of double-exchange (DE) ferromagnets. The double-exchange refers to a double electron exchange between neighboring Mn and O. This affects the Mn-O-Mn bond angle, and hence, the crystal structure. Here, M_x can be Ca, Sr or Ba. The large change in properties occurs near x=0.3 in composition with LaMnO₃ behaving as an insulator at one extreme of the compositional variation. Recent progress in the manufacturing of these perovskite has been achieved. The NEC -JAXA can now produce

various alternatives as (La,Sr) MnO₃ and of (La,Ca) MnO₃ and a compound (La,Sr,Ca) MnO₃ with better optical performance. They can prepare these materials in three forms, 'Bulk type' using standard ceramic techniques, 'Thick film type' by a printing method, and 'Thin film type' by synthesis of sol-gel [Tachikawa 2009]. The metal-insulator transition in this system is from an insulating state that has high optical absorption in the UV/VIS, to a semi-metallic reflective state.

Experimental work on the use of LaSrMnO₃ for smart thick-film radiation devices (SRD) has demonstrated variation in the thermal emissivity from 0.2 near 150 K to 0.6 above 300 K. The material was formed as a 10-20 μm tile that is subsequently attached to the space structure. The updated results of the LaSrMnO₃ showed a low solar absorptance [Nakamura 2006, Tachikawa 2009]. The results obtained with the LaSrMnO₃ are similar to those obtained with the VO₂

Electrochromic structures based on WO₃ [Granquist 1998, Franke 2002] employ an active switching mechanism involving the electric-field induced motion of group 1 ions, such as H⁺ or Li⁺. The resulting reactions convert the WO₃, which is IR transparent, to HWO₃ (or LiWO₃) complexes that are metallic and reflective in the IR. The device uses a multi-layer structure; consisting of a polymer that acts as a storage reservoir for the H⁺ or Li⁺-ionic colorant, an intermediate solid or liquid electrolyte to facilitate field-induced migration of the colorants, and the active WO₃ layer. The layers are sandwiched between two electrodes such as ITO. The transition from an insulating to a metallic state is controlled by the application of a voltage to enhance the diffusion of the colorant ions from the storage medium to the WO₃ layer. Trapping of the colorant ions tends to reduce the variation in the coloration characteristics of the WO₃-based electrochromic devices after a few hundred cycles.

Electrochromic technique can theoretically produce a large change in the IR reflectance. They are becoming commercially available (at the prototype level), although it has a relatively complex structure of at least 5 layers that entail different fabrication procedures.

Solid-state electrochromic structures are being developed (a-WO₃/a-Ta₂O₃/c-WO₃ [Franke 2002]) using Ta₂O₃ as a solid-state electrolyte. Moreover, the emissivity switching is based on ion motion (Li or H) and has a relatively slow response time that quickly degrades at the lower temperatures that can be encountered in space. The space environment also includes energetic protons and other ions that could react with the dangling bonds in the WO₃ and act as undesired colorants reducing the switching capability of the device. Franke et al. in a collaboration between the Universities of Nebraska-Lincoln (USA) and Leipzig (Germany) used the ZnSe to increase the solar reflectance of the electro-chromic WO₃ based tuneable radiator. The modeling of the multi-stack

showed excellent reflection, but no further experimental published work could be found.

Recent interests were revived by some applications where the electrochromic could be the most suitable such as for the astronaut suits in extra-vehicle activities (EVA) [Metts 2009]. Such applications do not require high number of switching (one switch/activity), and only a small fraction of ions are trapped and the performance is still acceptable. The WO₃ based electrochromic device is flexible and its manufacturing technology is relatively mature compared to VO₂ and LaSrMnO₃.

The VO₂-based smart material system exhibits several relatively unique characteristics for use in thin-film SRD's:

- **High density of free electrons above the metal-insulator transition temperature,**
- **The metal-insulator transition in VO₂ can be controlled passively by temperature through thermal generation of carriers (n(T)) or actively through electric-field induced band bending to generate a critical free electron density, n(V).**

The VO₂ system is relatively unique in that it can be employed as the basis of both passive thermochromic and active electrochromic devices.

Currently, MPB is focusing on the passive thermochromic structure. The opto-electronic switching characteristics of the VO₂ film can be tailored by doping with acceptors and donors, similar to the case of crystalline Si in microelectronics. This provides considerable leeway to optimize the SRD performance relative to competing technologies. The stoichiometric bonding to oxygen results in good AO and radiation resistance, comparable to SiO₂ AO protective coatings. The low solar absorptance that is intrinsically attainable with the VO₂-based coating results in a simpler, more cost-effective SRD structure.

In principle one can add as many interference based stack layers (e.g. VO₂/SiO₂) to increase the solar reflectance. However the IR tuneability will suffer from negative effects such as internal stresses that will develop within the IR tuneable layers and decrease the tuneability.

Another important aspect is the temperature range of the emittance tuning. Tuning at very low or very high temperatures is not desirable for SRD's. The optimal tuning range is between -10°C and +30°C

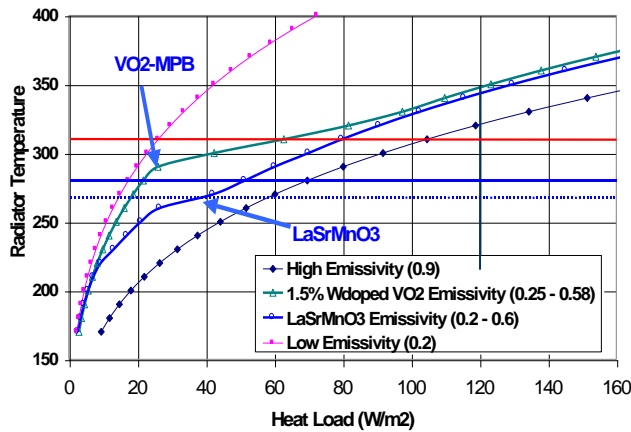


Figure 13: Comparison of the performance of a trial doped VO₂ SRD with published data for LaSrMnO₃ based SRDs.

Figure 13 illustrates the heat load dissipation of the VO₂-SRD, the LaSrMnO₃-SRD, and a high emittance radiator. The performance of the VO₂ and LaSrMnO₃ are very similar at high temperature. However, VO₂ allows for better thermal control at lower temperatures due to its higher transition temperature (Figure 14). The values of the LaSrMnO₃ emittance, used for the figure are from [Nakamura 2006, Fig. 2].

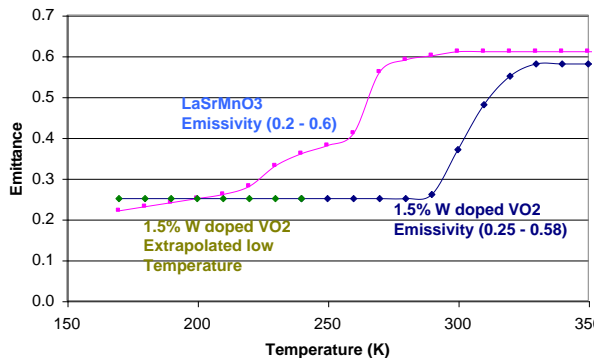


Figure 14: Emissivity profiles of the VO₂ and LaSrMnO₃ based SRDs.

7 OTHER APPLICATIONS OF VO₂

7.1 Hadamard Mask

Switching of VO₂ can be achieved by electrical charge injection (voltage) leading to the application as a smart Hadamard mask for spectrometers. The Hadamard technique replaces the single slit with a mask of n slits. A combination of n Open or Closed slits, respecting Hadamard conditions, is needed to solve the equations for the slits. Usually the masks are mechanically made and will be moving in front of the spectrometer entrance. VO₂ allows for a stationary mask where the individual slits are controlled by the reflecting/transmitting state of the VO₂ film. The Hadamard technique allows for an increase in

Signal/Noise ratio by a factor of about \sqrt{n} . Smart micro-slit arrays with 16 electrically controllable elements were patterned by the standard photolithography followed by plasma etching to build an electrically controllable smart VO₂-Hadamard array (Figure 15). A prototype shutter was tested at the input to MPB's IOSPEC miniature Infrared spectrometer verifying the increase in Signal to Noise ratio.

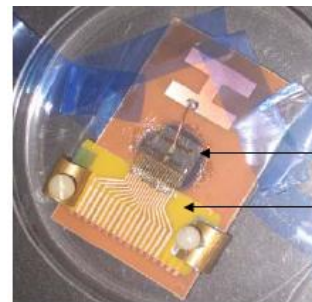
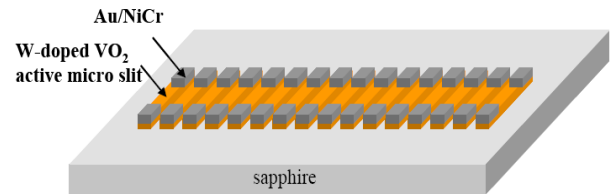


Figure 15: VO₂-Hadamard Shutter for the entrance of a spectrometer to increase the Signal/Noise ratio

7.2 Optical switch for telecom

All-optical switching of VO₂ was performed by a pump-probe technique combining a continuous wave diode laser beam at 980 nm for the photo-excitation of the film and a fibre laser beam at 1.55 μ m provided by a tunable laser source (Figure 16). The signal is transmitted when the film is in its semiconducting state and reflected when it is switched to its metallic state under photo-excitation by the pump laser beam at 980 nm. The extinction ratio between the semiconducting (on) and the metallic (off) state is approximately 20 dB [Soltani 2006].

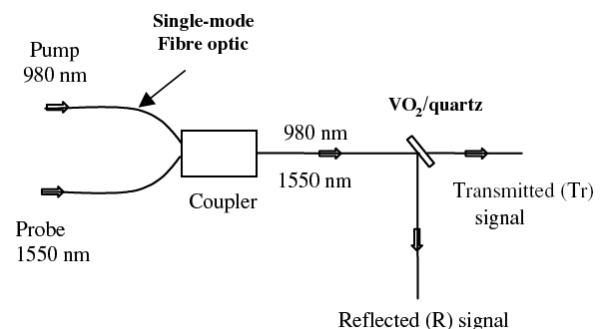


Figure 16: Scheme of the all-optical switching experimental set-up

7.3 ESD Protection

Electro-Static Discharge (ESD) and their effects on spacecraft were observed since the earliest geostationary satellites. At cryogenic temperature, non-conductive surfaces become dielectric with high surface resistivity, causing charge accumulation, mainly at the edges of antennas and structures [ECSS-E-20-06].

Thin film VO₂ with shallow W doping keeps sheet resistivity low at cryogenic temperature, providing protection against ESD, a main potential risk of large surface cracks in space [Haddad 2005].

Figure 17 compares the resistivity of the W-doped VO₂ thin film deposited on Kapton, with the current commercial sunshield. The MPB VO₂ film resistivity is three order of magnitude lower at -140°C to provide improved ESD protection at low temperatures.

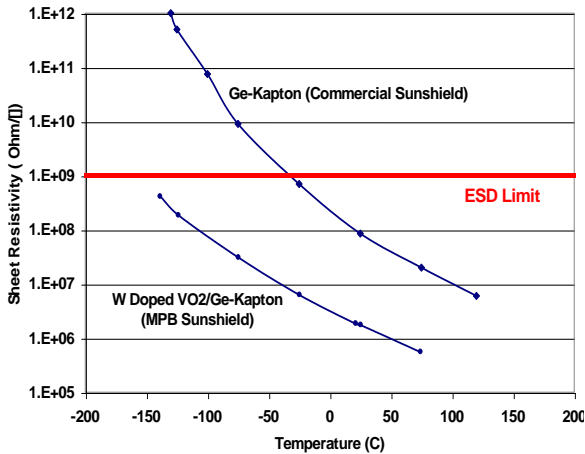


Figure 17: Comparison of the resistivity of the W doped VO₂ with the commercial sunshield for RF antenna

7.4 VO₂ film Flexibility

The flexibility VO₂ films further extends its application to larger domains such as a sunshield on Kapton for antennas or as a coating on astronaut suits in space manned mission (to help preserve the temperature inside the suit against outer temperature swings), and in Extra Vehicle Activities (EVA). NASA showed an interest for such applications and a US-team is working to develop an electrochromic coating for heat dissipation [Metts 2009].

In collaboration with EMS Technologies (now MDA) MPB has tested the flexibility of thin film VO₂ deposited on Kapton and Ge-coated Kapton [Haddad 2005]. As shown in Figure 18, the VO₂ coating is very flexible.

Table 10 summarizes the procedure for the VO₂/Kapton flexibility test. Six cylinders were used. The film was folded ten times over the cylinder and then inspected. The last test was destructive; the film was folded on itself and pressed 10 times. No cracks or film deformation was observed [Haddad 2005].

Table 10: Flexibility test summary.

Parameter	Values
Number of cylinders	6
Cylinder radius	25, 12.5, 6, 2.5, 1, 0.5 (mm)
Last test step	Fold the VO ₂ -kapton film on itself
Number of cycles	10 (for each radius)

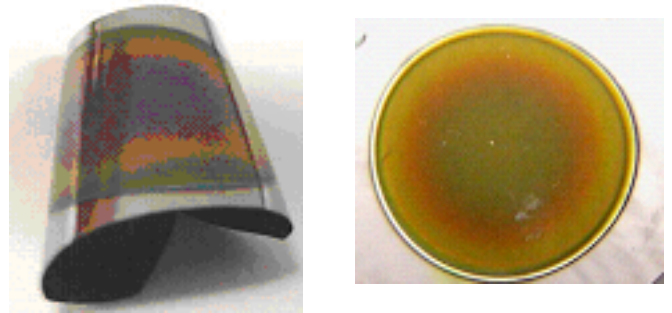


Figure 18: Flexibility of the VO₂ on Ge-Kapton sheet

CONCLUSIONS

MPB has developed, within CSA and ESA contracts, a novel thin film technology to improve the thermal management and heat dissipation of spacecrafts and their payloads. This technology is based on passive emittance tuneability of a VO₂ film in response to the temperature of spacecraft.

MPB is currently focusing on the development of a passive VO₂/SiO₂/VO₂ multilayer SRD. The best sample obtained has an emittance tuneability ($\Delta\epsilon$) of 0.36 (e-low = 0.38, e-high = 0.74), and a solar absorptance of 0.32. Thermal vacuum cycling (up to 4000 cycles) and thermal shock test (17 cycles between Liquid Nitrogen and 165°C) validated the stability of the emittance tuneability and solar absorptance.

MPB is considering, a flight experiment to demonstrate the technology in a space environment

and to validate its on-orbit performance. SRD monolayer coupons, fastened on a honeycomb base to simulate a small radiator, have successfully passed the non-destructive test series (vibration, thermal cycling, thermal shock). Other individual samples passed the Atomic oxygen and preliminary radiation tests. Peeling tests confirmed the strong adherence of the VO₂ coating to the Al substrate.

In the current study four multilayer SRD successfully passed thermal cycling and thermal shock tests with a slight reduction of the tuneability. They show the same stability as the monolayer VO₂.

Single layer VO₂ films have yielded broadband IR emittance tuneability of about 0.45. Using the SRD, with its current performance (tuneable emissivity between 0.35 and 0.8), the heat load range increases to 35-120W for a payload temperature range of 10-40°C; whereas an ideal SRD with a tuneable emissivity between 0.2 and 0.8, would further extend the heat load range to approximately 20 –120W. The extended operating range provided by the SRD reduces the power consumption required by heaters commonly used to control the payload temperature. Still higher performance is feasible through optimization of the nano-engineering process and the use of a multi-layer structure

ACKNOWLEDGEMENTS

The authors gratefully acknowledge the financial support of the Canadian Space Agency and the European Space Agency, as well as the constructive advice of Darius Nikanpour and Xin Xiang Jiang from CSA and Philippe Poinas from ESA.

REFERENCES

[Baum 2007] Baum et al., “4D Visualization of Transitional Structures in Phase Transformations by Electron Diffraction”; (Science 318, 788 (2007)).

[Beteille 98], Beteille F. et al.; “Optical switching in VO₂ thin films J. Sol-Gel Science and Technologies” vol 13, (1998), 915-921

[Birur 2001] Birur G. C. et al.; “Micro/nano spacecraft thermal control using a MEMS-based pumped liquid cooling system” Presented at SPIE conference on Micromachining and Micro fabrication, October 21-24, 2001 San Francisco, USA.

[Bitter 2003] “ Electrostatic Appliqué for Spacecraft Temperature Control”, Space Technology & Applications International Forum, Feb 2-5 2003

Edited by El-Genk, M. S, Publisher Melville, N.Y. : American Institute of Physics, 2003 AIP # 654

[Cavalleri 2001] Cavalleri A. et al.; “Femtosecond Structural Dynamics in VO₂ during an Ultrafast Solid-Solid Phase Transition” Physical Review Letters, vol. 87, 3 December 2001 paper # 237401

[Chudnovskii 1999] F.A. Chudnovskii et al.; “Electrical Transport Properties and Switching in Vanadium Anode Oxides: Effect of Laser Irradiation,” Phys. Stat. Sol. A, 172, (1999) p. 391.

[Dachuan 1996], Yin Dachuan et al; “Vanadium dioxide films with good electrical switching property”; + J. Phys. D: Appl. Phys vol 29 (1996) 1051-1057

[ECSS-E-10-03A], “Space engineering, Testing”, Section 5.1.6, “Humidity Test, equipment qualification”; 15 February 2002. Published by ECSS Secretariat, ESA-ESTEC, Requirements & Standards Division, Noordwijk, The Netherlands.

[ECSS-E-20-06] Space Engineering – Spacecraft Charging, Environment-Induced Effects on the Electrostatic Behaviour of Space Systems- (Draft v0.11 27/09/2004;) Published by ECSS Secretariat, ESA-ESTEC, Requirements & Standards Division, Noordwijk, The Netherlands

[ECSS-Q-70-04A] “Space product assurance, Thermal cycling test for the screening of space materials and processes”; (4 October 1999) Published by ECSS Secretariat, ESA-ESTEC, Requirements & Standards Division, Noordwijk, The Netherlands.

[ECSS-Q-70-13A] Space product assurance – Measurement of the peel and pull-off strength of coatings and finishes using pressure-sensitive tapes”, 4 October 1999, Published by ECSS Secretariat, ESA-ESTEC, Requirements & Standards Division, Noordwijk, The Netherlands.

[Egorov 1991a] Egorov F.A. et al.; “ Thin VO₂ films with high optical contrast ”; Sov. Tech. Phys. Lett. Vol 17 No 4 (1991)295-296

[Egorov 1991b] Egorov F.A. et al.; “ Optically controlled fiber optic switch based on a VO₂ film”; Sov. Tech. Phys. Lett. Vol 17 No 5 (1991) p 345-346.

[Egorov 1991c] Egorov F.A. et al.; “ Controllable fiber-optic light modulator based on vanadium dioxide ”; Sov. Tech. Phys. Lett. Vol 17 No 11 (1991) 817-819

[Franke 2002] E. Franke et al.; “Low orbit-protective coating for all-solid-state electrochromic surface heat radiation control device” Surface and Coating Technology 151-152, 285 – 288 (2002).

[Granquist 1998] C.G. Granquist et. Al., Solar Energy, 63, pp. 199-216 (1998).

[Gilmore 2004] D.G. Gilmore, Satellite Thermal Control Handbook, The Aerospace Corporation Press, El Segundo, California, 1994.

[Griffith 1974] C.H. Griffiths and H.K. Eastwood, J. Appl. Physics, 45, p. 2201-2206 (1974).

[Guinneton 2004] F. Guinneton, L. Sauques, J.-C. Valmalette, F. Crosa, J.-R. Gavarrri; “Optimized infrared switching properties in thermochromic vanadium dioxide thin films: role of deposition

- process and microstructure"; Thin Solid Films Vol. 446 (2004) 287-295
- [Haddad 2005] E. Haddad, R. V. Kruzelecky, F. Bussi eres and P. Markland, "Smart-film Sun Shield for SAR Membrane Antennas" Final Technical Report, CSA Contract, Report-DP712015, March 2005.
- [Haddad 2006] E. Haddad, R. Kruzelecky et al., "Multi-Function Tuneable Emittance Smart Coatings For Thermal Control In Harsh Space Environment"; ICES, 36th International Conference On Environmental Systems, July 11-14, 2006, Norfolk, Virginia, USA; Paper 2006-01-2263, October 21-24, 2001 San Francisco, USA.
- [Kruzelecky 2005] R. V. Kruzelecky, E. Haddad, W. Jamroz, M. Soltani, M. Chaker, D. Nikanpour, X. Jiang, and G. Colangelo, Thin-film Smart Radiator Tiles with Dynamically Tuneable Thermal Emittance"; Society of Automotive Engineers, Inc. Proceeding, Paper # 2005-01-2996; 35-ICES, July 11-14, 2005, Rome, Italy.
- [Magna 2008] Magna Steyr Inc (Austria); "Micro Electro-Mechanical Louvers for Thermal Radiators" ESA contract completed in 2008 .
- [Mahan 1975] Bruce A. Mahan, *University Chemistry*, 3rd Edition, Addison-Wesley Publishing, p. 685-743 (1975).
- [Metts 2009] J. G. Metts and D. M. Klaus; "Conceptual Analysis of Electrochromic Radiators for Space Suits"; 39th International Conference on Environmental Systems; July 12-16, 2009; Savannah, Georgia, USA ;Paper ICES 2009 2009-01-2570
- [MIL-STD-883] Military standard test methods for microelectronics; Method 1010.7 Condition C, and 1010.9.
- [Morin 1959] F. Morin, "Oxide which shows a metal-to-insulator transition at the neel temperature", Phys. Rev. Lett. 3, 34 (1959).
- [Nakamura 2006] Y. Nakamura, et al.; "In orbit test result of smart radiation device"; Report ISTS 2006-c-20 (Japan, Institute of Space & Astronautical Science)
- [Osiander 2004] Osiander, R.; Firebaugh, S.L.; Champion, J.L.; Farrar, D.; "Micro-electromechanical devices for satellite thermal control", Sensors Journal, IEEE; Vol. 4(2004) 525 - 531.
- [Petit C.] Petit C. et al.; "Hysteresis of the metal-insulator transition of VO₂; evidence of the influence of microscopic texturation "; J. Phys. : Condens. Matter. Vol. 11 (1999) 3259-3264.
- [Soltani 2006] M Soltani, M Chaker, E Haddad and R Kruzelecky, "1 × 2 optical switch devices based on semiconductor-to-metallic phase transition characteristics of VO₂ smart coatings", Meas. Sci. Technol. 17 (2006) 1052–1056
- [Stefanovich 2000] G. Stefanovich, A. Pergament and D. Stefanovich, J. Phys. Condens. Matter, 12, p. 8837-8845 (2000).
- [Tachikawa2009] S. Tachikawa, A. Ohnishi, K. Matsumoto, Y. Nakamura, A. Okamoto; "Multi-layer Coating for Smart Radiation Device with Solar Absorptance 0.13"; 39th International Conference on Environmental Systems; July 12-16, 2009; Savannah, Georgia, USA ; Paper ICES 2009-01-2574
- [Zener 1951] Zener C.; "Interaction Between the dpShells in Transition Metals, II. Ferromagnetic Compounds of Manganeses with Perovskite Structure", Physical review Vol. 82 No3 (1951) 403-405.